Peer-reviewed version available at Sustainability 2018, 10, 1072; doi:10.3390/su10041072

Article

Assessment of building damage risk by natural disasters in South Korea using decision tree analysis

KeumJi Kim [1], SeongHwan Yoon [2,*]

[1] Department of Architecture, Pusan National University, Pusan, Republic of Korea; keumjikim@gmail.com
[2] Department of Architecture, Pusan National University, Pusan, Republic of Korea; yoon@pusan.ac.kr
* Correspondence: yoon@pusan.ac.kr; Tel.: +82-51-510-2355

Abstract: Changes in extreme weather patterns are expected under climate change. In this study, a risk assessment was conducted using 4 building damage history datasets and 33 weather datasets (precipitation, wind speed, snow, and temperature) from 230 regions in South Korea to quantitatively analyze and predict building damage caused by potential future natural disasters. Decision tree analysis was used to evaluate building damage risk in 230 regions. The decision tree model to determine the risk of flood, gale, and typhoon was generated, which excluded gales, with less damage. The weight (variable importance) and limit value (damage limit) of the weather variables ware derived using the decision tree model. Using these two factors, we assessed the building damage risk in 230 regions in South Korea until 2100. The number of regions at risk of flood damage increased by more than 30% in average. Conversely, regions at risk of snowfall damage decreased by more than 90%. The regions at risk of typhoons decreased by 57.5% on average, and the number of regions at high risk of typhoon damage increased by up to 62.5% in RCP 8.5. These results can be used as objective data to minimize future building damage throughout South Korea, representing the first step towards sustainable development in the region with respect to disaster response.

Keywords: building damage; climate change scenarios; decision tree analysis; limit value; natural disaster; random forest; risk assessment process; South Korea

1. Introduction

Since the 1950s, changes in extreme weather have been observed, with decreases in cold temperature extremes, increases in warm temperature extremes, increases in high sea levels, and increases in the number of heavy precipitation events [1]. Such changes in climate are projected to increase the risks for people and assets in urban areas due to heat stress, storms and extreme precipitation, inland and coastal flooding, landslides, air pollution, drought, water scarcity, sea level rises, and storm surges [2].

The occurrence of natural disasters has steadily increased since 2000, but the number of disasters has reportedly decreased in recent years [3]. However, the number of people directly or indirectly affected by disasters and the associated costs are increasing [4]. 2016 experienced the third-lowest number of natural disasters since 2006, which was below the annual average disaster occurrence for 2006–2015. However the number of people affected by natural disasters in 2016 (569 million) was the highest since 2006 [3].

Asia and the Pacific are the most disaster-prone regions in the world [5]. In particular, developing countries in Asia are vulnerable to extreme weather events under present-day climatic variability [6]. According to an Economic and Social Commissions for Asia and the Pacific report [7], 47% of the world's 334 disasters have occurred in Asia. In addition, the number of deaths in South Asia has accounted for 64% of all deaths. This is caused in part by the fact that developing countries in Asia are vulnerable to extreme weather events due to climate change. In addition, developing

countries are increasingly suffering from inadequate equipment (e.g., old buildings and unsafe facilities) that cannot survive weather changes [8]. However, damage from natural disasters can occur at any time, depending on the region and environment, including in developing countries. As a result, precautions and countermeasures should be implemented to reduce the magnitude of damage and to prevent unpredictable disasters.

Buildings are the main space in which humans live. In the event of a disaster, damage or collapse of buildings leads to injury and deaths. Therefore, quantitative analysis of building damage caused by natural disasters can help reduce future damage and economic losses. Therefore, in recent years, studies have been attempted to analyze the causes and consequences of building damage caused by natural disasters.

Blong et al. [9] analyzed the effects of natural disasters on residential building damage in Australia and analyzed the impacts and problems caused by natural disasters. Floods, tropical cyclones, thunderstorms, bushfires, landslides, earthquakes, and tsunamis are particularly hazardous for residential buildings. Moreover, studies have indicated that hail presents the greatest risk of damage to buildings from natural disasters, but there are no regulations to prevent damage to buildings. To develop and verify building damage assessment methods applicable to earthquake and storm risks around the world, Chandler et al. [10] set the parameters associated with the building structure (e.g., building age, building height, and occupancy) and proposed an evaluation method using vulnerability curves. Various other data have been used in building disaster evaluations, such as the number of floors and construction type [11]. Meanwhile, Yazdani et al. [12]. Collected data on building damage caused by natural disasters based on a field survey and estimated the cause and magnitude of damage based on the structural characteristics. Moreover, Luo et al. [13] analyzed the relationship between gale speed and building damage to reconstruct the gale field around the damage to a residential building after a typhoon. Based on this, they suggested the possibility of constructing a model according to other disasters. Pita et al. [14] presented a new approach to assessing damage to building interiors caused by hurricanes using the Florida Public Hurricane Loss Model. Finally, Renou et al. [15] proposed a geographic information system (GIS)-based assessment method to assess building vulnerability and damage in the event of a tsunami. Based on past disaster data, they conducted an assessment of residential buildings and local risks in the Moroccan coastal zone and created a map of building damage.

Furthermore, various analytical methods such as probabilistic analysis [16] and Monte Carlo simulation [17-19] have been used to evaluate building damage caused by natural disasters [20]. In recent years, researches have used artificial intelligence such as data mining and machine learning for the identification and evaluation of risk factors of natural disasters. These methods present a systematic and automatic way to find statistical rules and patterns from large amounts of data. To study natural disaster risk, various techniques have been studied, such as artificial neural network [21-23], support vector machine [22,24], and Bayesian network and clustering. In addition, Liu et al. [25] proposed statistical model parameters of compact polarimetric synthetic aperture radar. Finally, Reese et al. [26] assessed building vulnerability using logistic regression for damage data collected during the 2009 South Pacific tsunami and verified the disaster vulnerability factors by building use.

The damage to buildings by natural disasters is affected by various factors, such as weather conditions, the environment in which buildings are located, and building structure. Easterling et al. [27] argued that if there are identifiable trends in extreme climatic events such as temperature or precipitation, human impacts on climate change are a very important factor of damage from natural disasters. Spekkers et al. [28] investigated the mechanism of storm damage occurrence and the relationship between this mechanism and meteorological variables. The results showed that the maximum flood intensity and precipitation were predictive factors for the probability of precipitation. However, few studies have attempted quantitative analysis focusing on the weather conditions and building damage.

Therefore, in the present study, weather conditions were used as the variables to assess the building damage risk. For this analysis, decision tree analysis was used to identify the causes of

natural disasters and building damage. Decision tree analysis generates decision support rules for various phenomena as a method of machine learning, and is useful for evaluating various risks to humans and the environment when the expected utility model indicates the risk that cannot be represented [29]. Many studies have evaluated the risk of natural disaster using decision tree techniques [30,31]. For example, Guo et al. [30] used classification and regression tree partitioning rules to identify flood hazards in 35 catchments in 10 regions in China. The decision tree technique can outperform other regionalization approaches, because it generates rules that optimally consider spatial proximity and physical similarity. Moreover, the random forest classification function of the decision tree can be efficiently executed for large databases, and it is possible to derive the importance of specific variables among classifications [31]. For example, Quanlong et al. [32] classified remote sensing images using a random forest classifier as the main method for flood mapping in China and extracted flooded areas with a 94% accuracy.

The purpose of this study is to analyze the impact of weather conditions on building damage and evaluate the risk in South Korea, as well as predict future building damage using climate change scenarios. For this purpose, we assessed the building damage risk using decision tree analysis, which can generate the importance of each variable and decision rules.

2. Methods and data

2.1. Methodology

This study used observation weather data, climate change scenarios, and building damage history as the input data. Correlation analysis and decision tree analysis, which is a data mining technique, were used for the building damage risk evaluation. Decision tree analysis is a useful method for predicting the results of future records using tree models derived from historical data [33]. The spatial unit for evaluating building damage effects and prediction were based on 230 administrative districts of the Republic of Korea. Each administrative district operates as a separate autonomous region, and in cases of damage caused by natural disasters, regional disaster management is performed. Therefore, this division was appropriate for predicting and analyzing the building damage risk in Korea. The study period was from 2005 to 2014.

This study used three stages to evaluate building damage caused by natural disasters in 230 regions (see Figure 1). In the first stage, 33 weather indices and 4 building damage history indices were collected and verified as the input variables. Weather and building damage data were constructed based on the same time and location (2005–2014 and 230 regions in South Korea). The input variables in the decision tree model for the risk assessment were selected using correlation analysis.

In the second stage, the decision tree model was established using the selected input variables and the accuracy of the models was determined. Weights and limit values for the input variables were derived from the tree model with a low error rate. The weight indicates the importance of each variable, and the limit value represents the minimum limit value of the input variable to detemine whether a building is damaged. Building damage risk by regions was determined using the weights and limit value.

In the third stage, building damage in the 230 regions was compared and analyzed according to climate climate scenarios (representative concentration pathways (RCPs) 2.6, 4.5, 6.0, and 8.5), in which the derived weight and limit value derived from the decision tree model were employed for the risk calculation.

Preprints (www.preprints.org) | NOT PEER-REVIEWED | Posted: 12 February 2018 doi:10.20944/preprints201802.0087.v1

Peer-reviewed version available at Sustainability 2018, 10, 1072; doi:10.3390/su10041072

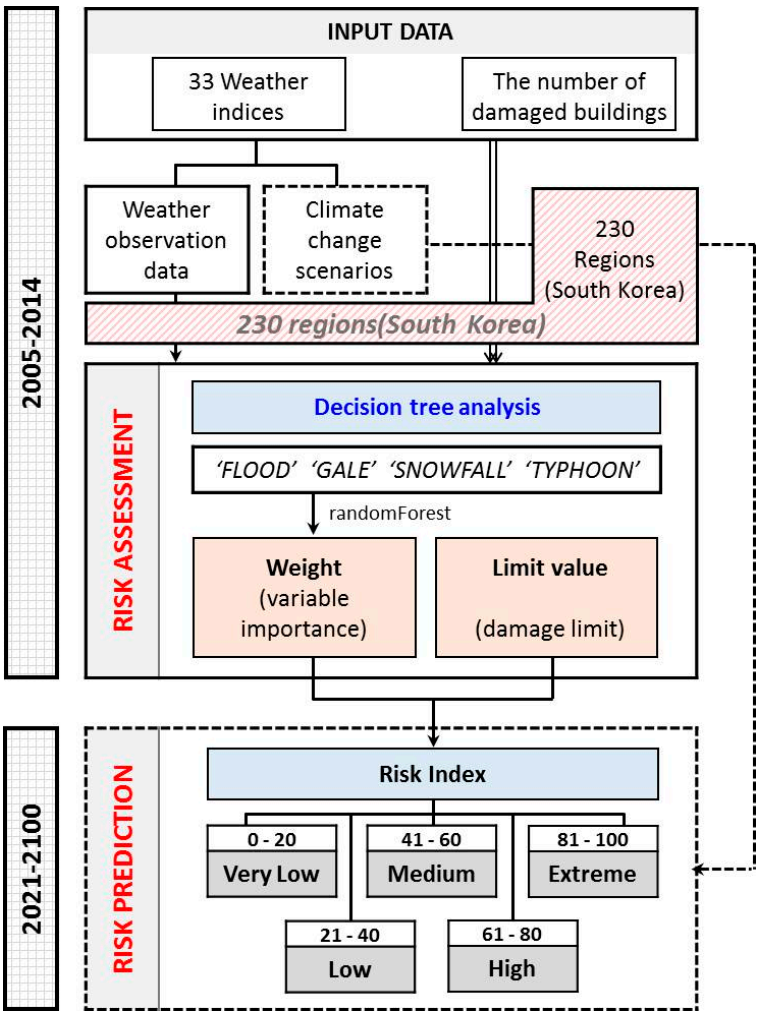

Figure 1. Schematic of the methodology

2.2. Decision tree analysis

This study used decision tree analysis to predict building damage risk. Decision tree analysis is defined as a classification procedure that divides a dataset into smaller subdivisions on the basis of a test set defined at each branch or limit value in the tree [34]. The decision tree model predicts outputs using given inputs [35] and generates rules for the entire area by repeatedly dividing the area of each variable. Generating rules with the decision tree analysis has the advantage of being easy to understand because of its logical "if–then" format and accessible implementation with simple database language such as structured query languages [36]. The decision tree analysis uses limit values as the criteria for its data classification.

The Gini Impurity in each tree is used to evaluate the relative importance of the input variables and evaluate the impact on the model [33], where the Gini Impurity is an indicator that determines if the data has been appropriately separated [37]. The Gini Impurity becomes 0 when the p value is equal to 0 or 1, and reaches a maximum in its parabolic distribution at a p value of 0.5. Overall, the accuracy increases as the Gini Impurity value decreases.

Using the decision tree model derived from historical data to predict the outcome of future is one of the most important roles [33]. In this study, we estimated the building damage risk by 2100 using a tree model derived from observation weather data and building damage history data. The weight and limit value of building damage was derived based on weather factors using the method described in section 2.1. The random forest function was used to derive the weights according to each input variable. The random forest is an ensemble method using a tree type classifier. It determines a partition of each limit value by searching a subset of randomly selected input

Preprints (www.preprints.org) | NOT PEER-REVIEWED | Posted: 12 February 2018 doi:10.20944/preprints201802.0087.v1

Peer-reviewed version available at Sustainability 2018, 10, 1072; doi:10.3390/su10041072

variables [38]. The accuracy of random forest has been examined in a number of studies that used it to derive the importance of variables [32,39,40]. For example, Gislason et al. [38] compared land cover classification using random forest and other ensemble methods (bagging and boosting), and showed that random forest outperformed other statistical models because it could assess the significance of variables.

This method of datafication can generate criteria for deciding output variables through an iterative process, which is the main feature of the decision tree model. The collected data from the input variables were datafied using the same criteria. Data were divided into the 'train set' and 'test set' in a 7:3 ratio to evaluate the model performance. Overestimation was determined by testing the flood set using the k-fold cross-validation method. The test set of the model was predicted using the 'predict' function. The weight and limit value of the input variables were derived from the decision tree model with the highest accuracy, and these two factors were used to predict future building damage (see Figure 2).

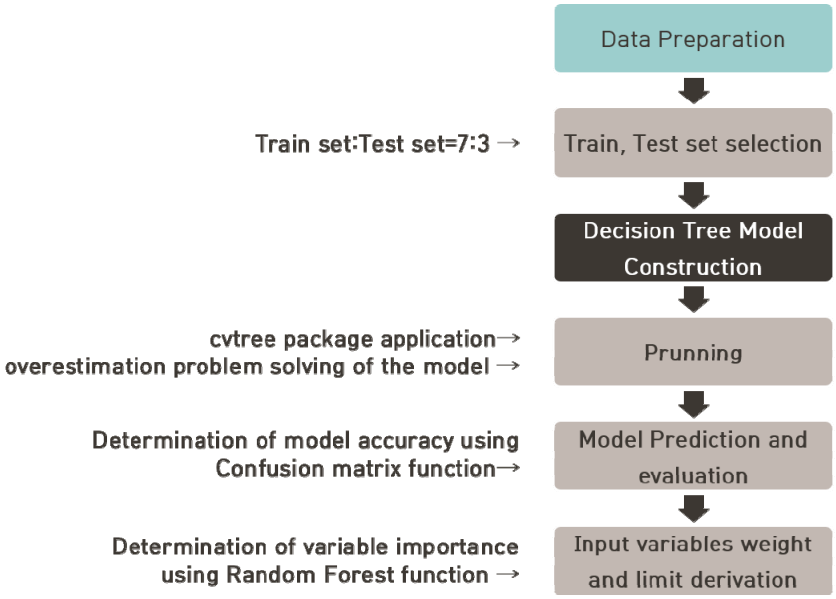

Figure 2. Process of decision tree analysis

2.3. Case study area

South Korea, a peninsula located in northeast Asia, was used as the case study for this research. The country is connected to the Asian continent in the north and is surrounded by the North Pacific Ocean (see Figure 3). It has an area of 9,972,000 ha as mainland and 3,330 islands. It is largely divided by natural barriers, such as mountains and rivers into three distinctive regions: the northern, central, and southern regions. South Korea is divided into 17 administrative districts consisting of one special city, six metropolitan city, and eight provinces.

Due to seasonal influences and its complex terrain, Korea experiences a unique climate. South Korea has four distinct seasons: spring, summer, autumn and winter. Abnormal dryness often occurs in spring, and cold temperatures often affect crops and human lives in spring. In summer, which starts in June, the humidity is very high, heavy flooding and typhoons (three or more per year) are frequent, and flood damage is an annual occurrence, especially in lowlands. The average annual precipitation is 1,200~1,500 mm in the central region, 1,000~1,800 mm in the southern region, 1,500~1,800 mm in Jeju Island, and 1,800 mm in the southern region, and 5~60% of annual precipitation is concentrated in summer. The highest temperature daytime temperature exceeds 30 °C, which causes frequent casualties due to urban heatwaves. Autumn is the most mild season due to the effects of high pressure systems, and there are relatively few natural disasters in autumn. Winter is cold and dry due to continental high pressure. However, since the amount of snowfall differs among regions, large differences in human and property damage exist by region.

Preprints (www.preprints.org) | NOT PEER-REVIEWED | Posted: 12 February 2018 doi:10.20944/preprints201802.0087.v1

Peer-reviewed version available at Sustainability 2018, 10, 1072; doi:10.3390/su10041072

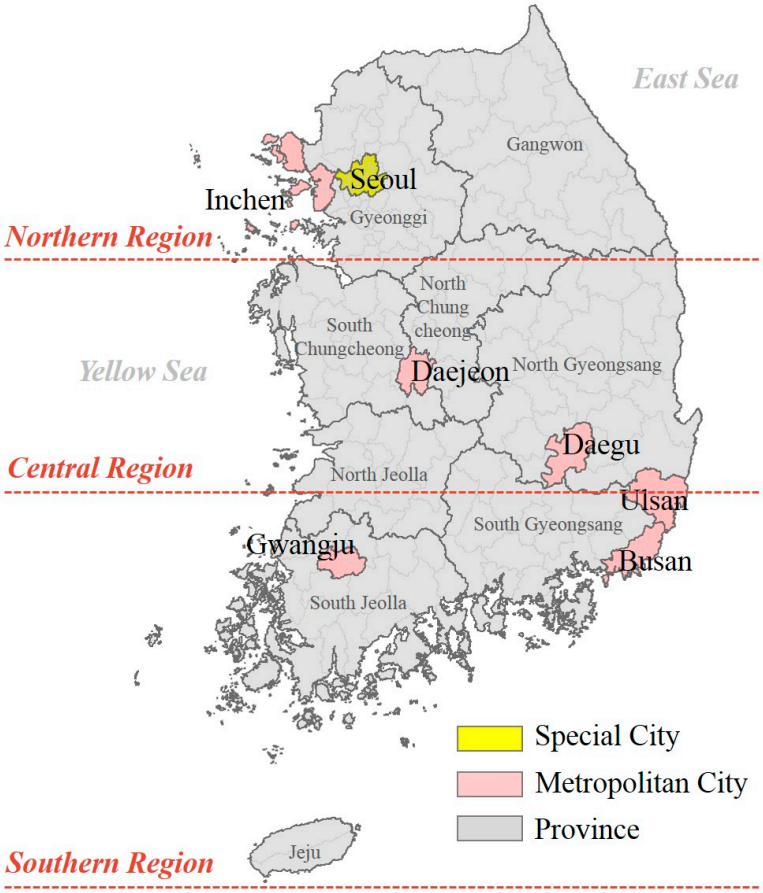

Northern Region: N
Central Region : C
Southern Region : S

	Name	
Special City	Seoul	N
Metro politan	Inchen	N
	Daegu	C
	Daejeon	C
	Busan	S
	Gwangju	S
	Ulsan	S
Province	Gwangwon	N
	Gyeonggi	N
	North Jeolla	C
	South Chungcheong	C
	North Chungcheong	C
	North Gyeongsang	C
	South Jeollan	S
	South Gyeongsang	S
	Jeju	S

Figure 3. Study area

2.4. Data

2.4.1. Weather

The weather data used in this study were observation weather data and climate change scenarios (see Table 1). Observation weather data from 2005 to 2014 were used to evaluate past building damage in Korea and the climate change scenarios for 2021 to 2100 were used to predict future building damage based on past building damage. Both observation weather data and climate change scenarios were used to assess building damage by natural disasters based on the 230 regions in South Korea. In other words, the building damage for the next 80 years was predicted via the evaluation of building damage in Korea in the past 10 years.

Table 1. Weather data

Weather data	Period	Space	Data	Purpose
observation weather data	2005-2014 (10 years)	230 regions	33 indices	Building disaster Assessment in the *Past*
climate change scenarios (RCP 2.6, 4.5, 6.0, 8.5)	2021-2100 (80 years)			Building disaster Prediction in the *Future*

The reprocessed climate change scenarios calculated by the Korea Meteorological Administration were used as weather data to assess and predict the damage caused by natural disasters in Korea. The intensity and frequency of natural disasters has been increasing, and there is a limit to producing detailed weather data using only a global climate model [42]. Therefore,

Preprints (www.preprints.org) | NOT PEER-REVIEWED | Posted: 12 February 2018 doi:10.20944/preprints201802.0087.v1

Peer-reviewed version available at Sustainability 2018, 10, 1072; doi:10.3390/su10041072

detailed weather data using regional climate models (RCMs) are essential for assessing natural disaster damage by region. Recent studies have shown that it is necessary to research how to decrease the scope from a global climate model scale to a finer spatial scale [43]. This study used detailed weather data calculated based on the regional climate. Table 2 shows the RCMs used to calculate weather data, the Hadley Centre Global Environmental Model ver. 3-Atmospheric regional climate model (HadGEM3-RA), the Regional Climate Model ver. 4.0 (RegCM4), the Seoul National University Regional Climate Model (SNURCM), and the Weather Research and Forecasting model ver. 3.4 (WRF) [42].

Table 2. Configurations of RCMs

	HadGEM3-RA	**RegCM4**	**SNURCM**	**WRF**
Institution	Korea Meteorological Administration	Kongju National Univ.	Seoul National Univ	Weather Research and Forecasting
Number of Grid (Lat.xLon.)	12.5km horizontal resolution			
	184*164	198*178	199*179	201*180
Vertical Coordination	38 hydrid	18 sigma	24 sigma	27 sigma
radiation	General 2-stream radiation	NCAR CCM3	CCM2 package	RRTM and Dudhia

[1] Table 2 were referenced in Kim, G et al. (p. 171)

Figure 4 presents the 230 spatial units of weather data. The weather data used in this study were reproduced from 73 automatic weather stations in Korea through objective analysis and interpolation [44] (p. 525). Since climate change scenarios use atmospheric model grid systems of regional climate models, they have a unique grid system, such as Lambert conformal or Mercator projection [45] (p. 519). However, in studies related to natural disasters, it is more efficient to use the GIS lattice system of administrative districts than Lambert conformal or Mercator projections [45] (p. 526).

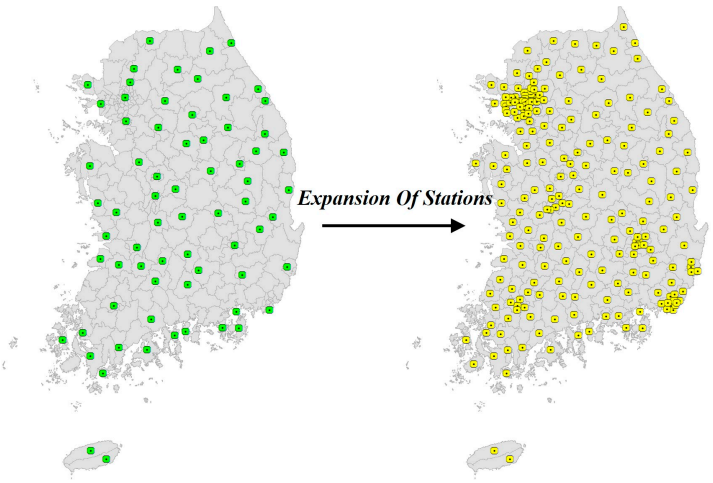

(**a**) Data by 73 Automatic weather station (b) data by 230 regions

Figure 4. Regions of weather data: (**a**) automatic weather stations in 73 regions; (**b**) weather observation stations in 230 regions.

However, detailed weather data using regional climate models have limitations in estimating the reliability of future forecasts due to errors and uncertainties [46]. The weather data used in this study were compared with regional precipitation on July 8, 2005. The automatic weather data and detailed weather data showed the same results; therefore, the data were judged to be reliable [47].

The data were generated after bias correction of the weather observations in the 230 regions. Since bias correction is based on observation data and modifies weather data, it has the advantage of reducing the uncertainty of the model results [48]. The data were divided into a single disaster index and a complex disaster index. The single disaster index consisted of 32 indices, including precipitation, temperature, gale speed, and snowfall, for the prediction of natural disaster damage. Korea is particular vulnerable to typhoons accompanied by heavy flooding and gales [44]. The complex disaster index is based on the precipitation and gale speed on the day of the typhoon, and consists of seven indices. All indices use an annual unit, and precipitation days are defined as days when precipitation exceeds 1 mm.

Table 3 lists the weather data indices, and Figure 5 presents the maps of the weather conditions in the 230 regions in 2005–2014. The average values of the precipitation indices 'sum_pr' and 'max_pr' (see Table 3 for full explanation of the weather index abbreviations) during 2005–2014 were 1,401.9 mm and 132.4 mm, respectively. High precipitation was mainly observed in the southern (Gyeongnam and Jeonnam Provinces) and northern (Seoul and part of Gyeonggi) regions. The average values for the snowfall indices 'max_nsnd' and 'sum_nsnd' were 7.7 cm and 28.2 cm, respectively. Precipitation was mainly concentrated in the Jeonnam coastal area and part of Gangwon Province, which has an average altitude of 500 m above sea level. The average values for the gale indices 'max_wind' and 'ave_wind567' were 9.9 m/s and 2.1 m/s, respectively. This showed that strong gales were mainly observed in the coastal area in Jeollanam Province and mountainous areas of Busan and Gangwon Province.

Future climate change impacts (short-, mid-, and long-term) were investigated for the RCP 6.0 scenario using the same weather indices. RCP 6.0 assumes that greenhouse gas reduction policies have been implemented to some extent. This scenario portrays larger socio-economic growth than that of the Special Report on Emissions Scenarios through the introduction of new and high-efficiency technology as well as a balance of fossil and non-fossil energy sources. For the precipitation index in RCP 6.0, the average 'max_pr' was 133.2–160.2 mm (after 2021), while the average 'sum_pr' was 1,327.4–1,397.3 mm (after 2021). Precipitation was found to increase in the 'short-term' to 'long-term' compared with the past. The snowfall index for the period after 2021 showed an average 'sum_nsnd' of 5.9–9.7 cm and the 'max_nsnd' was 2.5–3.5 cm, showing a very low snow compared to the previous period. A significant difference between the past and future gale indices was not observed as indicated by a 'max_wind' average of 9.8–10.0 m/s after 2021 and an 'ave_wind567' of 2.06–2.08 m/s.

Preprints (www.preprints.org) | NOT PEER-REVIEWED | Posted: 12 February 2018 doi:10.20944/preprints201802.0087.v1

Peer-reviewed version available at Sustainability 2018, 10, 1072; doi:10.3390/su10041072

291

Table 3. Weather Indices

A Single Disaster Variables			
Precipation	*max_pr*	mm	Annual maximum precipitation
	sum_pr	mm	Total annaul precipitation
	sum_jjapr	mm	Total annual precipitation during summer
	ave_gt80	mm	Average of more than 80mm precipitation
	px5d	mm	Greatest 5 day total flood
	days_wetday	days	Number of days with precipitation
	Pint	mm	Simple daily intensity
	Pxcdd	days	Max number of consecutive dry days
	ave_drydays	days	Number of average consecutive dry days
	pq90	mm/day	90th percentile of floodday ammounts
	pnl90	days	Number of events>long term 90th percentile
	pfl90	%	Percent of tatol flood from events>long-term 90th percentile
	days_gt80	days	Number of days more than 80mm precipitation
	days_gt160	days	Number of days more than 160mm precipitation
Snow	*ave_nsnd*	cm	Average of fresh snow cover
	sum_nsnd	cm	Sum of fresh snow cover
	max_nsnd	cm	Max of fresh snow cover
	days_nsnd5	days	Number of days more than 5cm fresh snowcover
	days_nsnd20	days	Number of days more than 20cm fresh snow cover
	days_nsnd50	days	Number of days more than 50cm fresh snow cover
Temperature	*days_freez*	days	Number of days below 0℃
	ave_maxtemp	℃	Daily minimum temperature
	ave_mintemp	℃	Daily maximum temperature
Wind speed	*days_mwind14*	days	Number of days more than 14m/s maximum velocity
	ave_wind567	m/s	Average wind velocity during May-July
	max_wind	m/s	Maximum wind speed
Complex Disaster Variables			
FLOOD	© *days_wetday*	days	Number of days with precipitation
	© *pint*	mm	Simple daily intensity
	© *max_pr*	mm	Annual max precipitation
	© *sum_pr*	mm	Annual sum precipitation
GALE	© *days_mwind14*	days	Number of days more than 14m/s maximum velocity
	© *ave_wind*	m/s	Average wind velocity
	© *max_wind*	m/s	Maximum wind speed

292
293
294

Preprints (www.preprints.org) | NOT PEER-REVIEWED | Posted: 12 February 2018 doi:10.20944/preprints201802.0087.v1

Peer-reviewed version available at Sustainability 2018, 10, 1072; doi:10.3390/su10041072

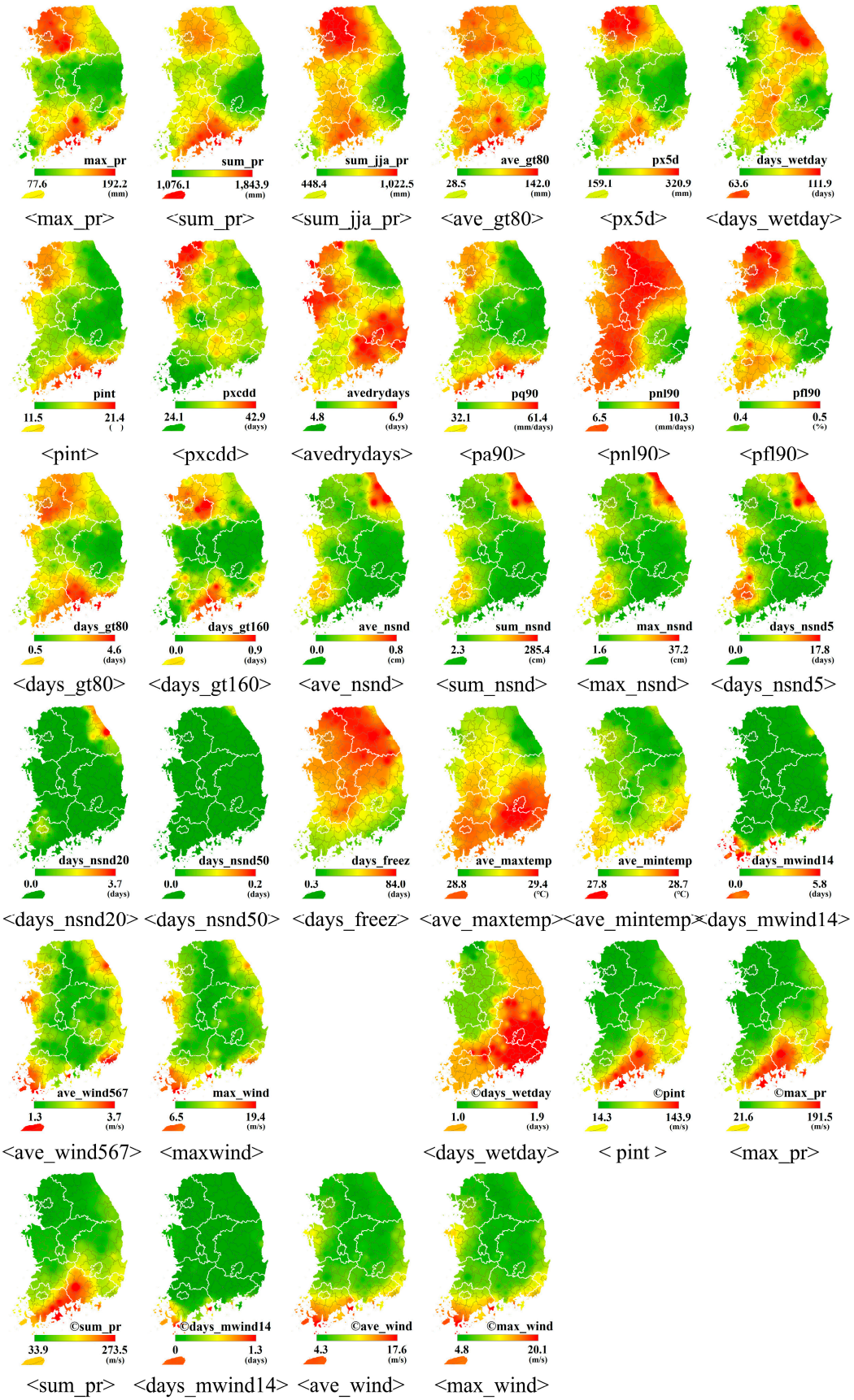

Figure 5. Weather conditions (2005–2014)

Preprints (www.preprints.org) | NOT PEER-REVIEWED | Posted: 12 February 2018 doi:10.20944/preprints201802.0087.v1

Peer-reviewed version available at Sustainability 2018, 10, 1072; doi:10.3390/su10041072

2.4.2. Building damage history

We used building damage history data with the function as the dependent variables in the annual disaster reports of the Republic of Korea. It was constructed for the same periods and space unit as the weather data. The annual disaster report is the natural disaster damage data issued annually by the administrative authority of the Republic of Korea. It records details of buildings, facilities, and loss of lives caused by natural disasters in Korea for one year from January 1 to December 31. These data were considered to be appropriate for the objective comparison of disasters in the 230 regions of Korea. The annual disaster reports provide information on are flooded areas, buildings, ships, farmland, public facilities, and private facilities. In this study, the total sum of missing/destroyed, partially damaged, and flood buildings was used. The four types of natural disasters that contributed to building damage during 2005–2014 were flood, gale, snowfall, and typhoons. Therefore, these four types of natural disasters were used for the building risk assessment in this study.

In total, 87,446 buildings over the past 10 years incurred flood damage in South Korea, costing approximately USD 90 million. Additionally, there were 80 reported cases of gale damage, 439 reported snowfall damage cases, and 15,115 reported typhoon damage cases. Since building damage caused by floods accounted for about 84.8% of the total damages, flood was confirmed as the natural disaster with the most significant effect on building damage. Additional damage incidences were caused by typhoons (14.7%), snowfall (0.4%), and gale (0.1%). According to building damage patterns for each natural disaster type, about 97.5% of the total damages caused by flood originated from flooding. Partial building damage was found in more than 80% of the total damages caused by snowfall and gale. In the case of typhoons, about 82% of the total damages were flood-related, and 14.8% of the incidences were partial building damage.

Figure 6 shows the amount of damage in each region. The spatial characteristics showed that flood damage was concentrated in the southern and northern regions (Seoul, Gyeonggi, and Gangwon). Damage caused by snowfall was concentrated in the coastal area of South and North Jeolla and Gangwon Province. In the case of typhoons, damage was mainly observed in southern regions (Gyeongnam and South Jeolla Province).

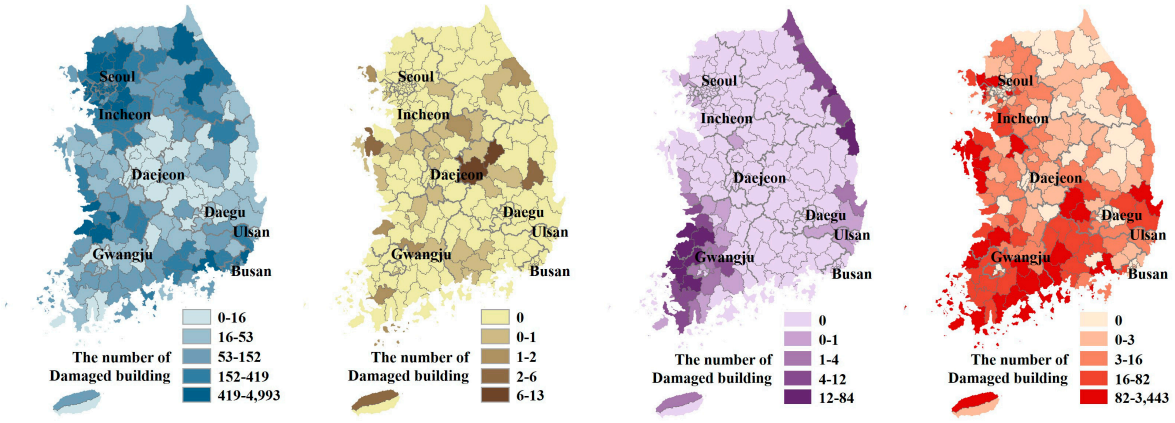

(a) **Flood** (b) **Gale** (c) **Snowfall** (d) **Typhoon**

Figure 6. Buildings damaged by natural disasters (2005–2014)

Preprints (www.preprints.org) | NOT PEER-REVIEWED | Posted: 12 February 2018 doi:10.20944/preprints201802.0087.v1

Peer-reviewed version available at Sustainability 2018, 10, 1072; doi:10.3390/su10041072

3. Results

3.1. Input Variables Selection

To apply weather indices with a high impact on the input variables for the model, a correlation analysis was performed before constructing the decision tree model. The correlations of the 14 precipitation indices of flood damage, 6 snow indices of snowfall damage, 3 wind speed indices of gale damage, and 7 indices (including precipitation and wind speed) of typhoon damage were evaluated. The results are shown in Tables 4.

The results showed that 11 precipitation indices, except for 'days_wetday', 'ave_drydays', and 'pnl90', were correlated with flood damage. In addition, five of the snowfall indices, except 'days_nsnd50', were highly correlated with snowfall damage. A high correlation with typhoon damage was found in six of the complex disaster indices, except for '©days_wetday'. Of the temperature indices, a high correlation was found with 'days_freez' and damage caused by floods and typhoons, 'ave_maxtemp' with flood damage, and 'ave_mintemp' with typhoon damage. Conversely, no correlation between gale indices and damage caused by gale was observed. Since there are relatively few annual disaster reports of gale damage compared to other natural disasters, its correlation for all indices was confirmed to be non-significant. The 13 flood evaluation indices, 5 snowfall evaluation indices, and 8 typhoon evaluation indices with high correlations were selected to determine the damage caused by flooding, snowfall, and typhoons. Consequently, these indices were used to establish the decision tree model.

Table 4. Correlations of the weather indices

Weather Indices	Building damage			
	Flood	Gale	Snowfall	Typhoon
max_pr	.3462**			
Sum_pr	.2309**			
Sum_jjapr	.3943**			
ave_gt80	.2076**			
px5d	.3393**			
days_wetday	-.1216			
pint	.2889**			
pxcdd	.3728**			
ave_drydays	-.0041			
pq90	.2778**			
pnl90	.1152			
pfl90	.4005**			
days_gt80	.2076**			
days_gt160	.3640**			
ave_nsnd			.2864**	
sum_nsnd			.2865**	
max_nsnd			.3053**	
days_nsnd5			.2925**	
days_nsnd20			.1827**	
days_nsnd50			.0215	
days_freez	.2864**	.4020	-.0932	-.3017**
ave_maxtemp	.2865**	-.0360	.0193	.1192
ave_mintemp	.3053**	-.0784	.0867	.3250**
days_mwind 14		.0744		
ave_wind567		-.0.335		
max_ wind		.0281		

Preprints (www.preprints.org) | NOT PEER-REVIEWED | Posted: 12 February 2018 doi:10.20944/preprints201802.0087.v1

Peer-reviewed version available at Sustainability 2018, 10, 1072; doi:10.3390/su10041072

© *days_wetday*				*.0059*
©*pint*				*.2622***
©*max_pr*				*.2349***
©*sum_pr*				*.3110***
©*days_mwind14*				*.5139***
©*ave_wind*				*.3769***
©*max_wind*				*.3539***

3.2. Assessment of building damage using decision tree analysis

3.2.1. Decision tree model accuracy

The accuracy of each model was compared and evaluated according to the building damage classification using 13 flood damage evaluation indices, 5 snowfall damage evaluation indices, and 8 typhoon damage evaluation indices, which were calculated using a correlation analysis based on the variables in section 4.1. The lower predictive ability of the decision tree analysis was calculated using a regression model with continuous output variables. Thus, model disadvantages could be overcome through conversion and categorization of variables in this study. The 'quantile' method, which is the classification method of the ArcMap, was used to set a similar frequency for each category (see Table 5).

Table 5. Classification of damaged buildings by natural disaster

Class	Flood		Gale		Snowfall		Typhoon	
	Building damage	Number of regions	Building damage	Number of regions	Building damage	Number of regions	Building damage	Number of regions
5	0-16	46	0	188	0	183	0	61
	17-49	46	1	29	1	17	1-3	47
	50-149	46	2	7	2-4	11	4-16	45
	150-403	46	3	3	5-12	10	17-82	39
	404-4993	46	4-13	3	13-84	9	83-172	38
4	0-25	58	0	188	0	183	0	61
	26-99	59	1	29	1	17	1-6	122
	100-326	57	2	7	2-6	17	7-51	54
	212-4993	56	3-13	6	7-84	13	52-1724	54
3	0-38	77	0	188	0	183	0-1	85
	39-211	77	1	29	1-3	26	2-21	75
	212-4993	76	2-13	13	4-84	21	22-1724	70
2	0-97	115	0	188	0	183	0-5	115
	98-499.	115	1-13	42	1-84	47	6-1724	115

Table 6 shows the accuracy and error rates based on the decision tree model. As the categories of buildings damage history data decreased, the model accuracy tended to increase. Among the flood damage prediction models (models R-1–4), model R-1 (two categories) showed the highest accuracy of 0.65. Meanwhile, model S-1 (two categories) had the highest accuracy of 0.85 among the snowfall damage prediction models (models S-1–4). In the case of the typhoon damage prediction model (model T-1–4), model T-1 (two categories) had the highest accuracy of 0.71. The model error rate (out-of-bag estimate of the error rate) simultaneously decreased in accordance with decreasing number of categories. Thus, the weight and limit value were derived from models R-1, S-1, and T-1, with two classifications, for flood, snowfall, and typhoon damage, respectively.

Preprints (www.preprints.org) | NOT PEER-REVIEWED | Posted: 12 February 2018 doi:10.20944/preprints201802.0087.v1

Peer-reviewed version available at Sustainability 2018, 10, 1072; doi:10.3390/su10041072

382 **Table 6.** Accuracy and error rate according to the decision tree models

Disaster	Tree model	class	accuracy	Error	Graph of misclass
Flood	Input Variables	day_gt80, day_gt160, pq90, px5d, pint, pxcdd, pfl90, ave_Gt80, max_pr, sum_pr, sum_jjapr, days_freez,			
	Model R-1	2	0.65**	26.5	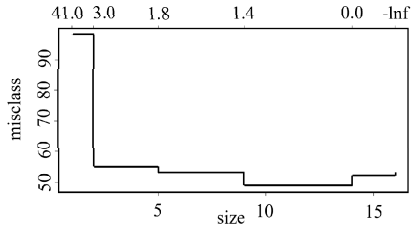
	Model R-2	3	0.56**	39.6	
	Model R-3	4	0.52**	53.4	
	Model R-4	5	0.29	31.3	
Snowfall	Input Variables	days_nsnd5, days_nsnd20, ave_nsnd, sum_nsnd, max_nsnd			
	Model S-1	2	0.85	17.4	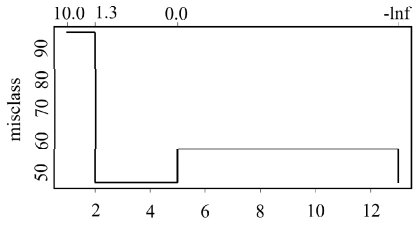
	Model S-2	3	0.79	22.6	
	Model S-3	4	0.81	22.6	
	Model S-4	5	0.78	23.0	
Typhoon	Input Variables	©pint, ©max_pr, ©sum_pr, ©days_mgale_14, ©ave_gale, ©max_gale, days_freez, ave_mintemp			
	Model T-1	2	0.71**	33.0	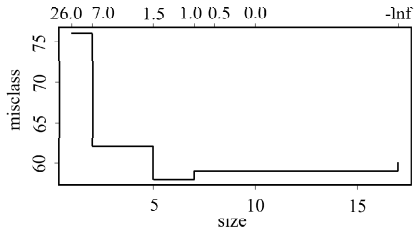
	Model T-2	3	0.55**	50.0	
	Model T-3	4	0.46**	58.3	
	Model T-4	5	0.36**	60.9	

383 [1] The size with the lowest 'misclass' value was fixed to the node's size of tree model.

384 3.2.2. Deriving the weight and limit value by input variables

385 The limit value and weight of the weather factors were derived based on damage caused by
386 each natural disaster scenario using decision tree model R-1 (flood damage evaluation model),
387 model S-1 (snowfall damage evaluation model), and model T-1 (typhoon damage evaluation
388 model), which showed the highest accuracies (see Table 7).

389 The weather factor with the highest impact on building damage caused by flood was 'ave_gt80',
390 while the level of impact followed the order 'sum_pr' > 'sum_jja_pr' > 'px5d' > 'max_pr'. According
391 to the weather factors that affected the risk of building damage caused by snowfall, the impact
392 followed the order 'sum_nsnd' > 'ave_nsnd' > 'max_nsnd'. In the case of typhoon damage, the
393 impact on building damage followed the order '©sum_pr' > '©max_gale' > '©ave_mintemp' >
394 '©days_freez' > '©max_pr' > '©ave_wind'.

395 In addition, the building limit value and the weight for each index were derived from the
396 decision tree model. The limit value for each model was used as the standard value to determine the
397 building damage category (high or low risk) for the output variables during the creation of the
398 decision tree model, and the building limit value was generated for each weather index.

399 It can be concluded that buildings in regions with a lower limit value than the average value in
400 2005–2014 are more likely to suffer from natural disaster damage in the future. In the flood damage
401 model (model R-1), the indices with a limit value lower than the average value during 2005–2014

Preprints (www.preprints.org) | NOT PEER-REVIEWED | Posted: 12 February 2018 doi:10.20944/preprints201802.0087.v1

Peer-reviewed version available at Sustainability 2018, 10, 1072; doi:10.3390/su10041072

were 'ave_gt80', 'sum_pr', 'px5d', 'max_pr', 'pfl90', 'pint', and 'ave_maxtemp'. For the snowfall damage model (model S-1), the 'max_nsnd' and 'days_nsnd5' indices had a lower 'limit value' than the average. Meanwhile, the '©ave_maxtemp', '©ave_mintemp', and '©ave_wind' indices in the typhoon damage model (model T-1) had a lower value than the average during 2005–2014.

Table 7. The weights and limit values based on the decision tree model

Variables	Weight	Limit value	Mean decrease accuracy&Gini
Model R-1			
ave_gt80	16.03	97.56 mm	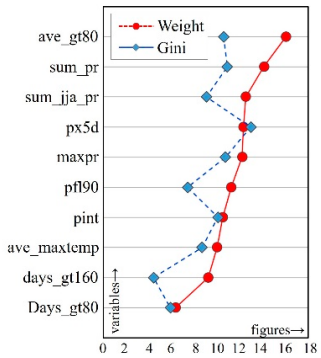
sum_pr	14.09	1344.90 mm	
sum_jjapr	12.80	961.10 mm	
px5d	12.30	217.38 mm	
max_pr	12.19	104.83 mm	
pfl90	11.22	0.43%	
pint	10.48	17.01 mm	
ave_maxtemp	9.98	29.10 ℃	
days_gt160	9.21	0.35 days	
days_gt80	6.32	2.00 days	
			(a)
Model S-1			
sum_nsnd	26.20	69.7 cm	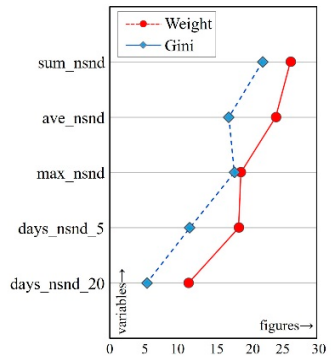
ave_nsnd	24.06	0.12 cm	
max_nsnd	18.98	7.15 cm	
days_nsnd5	18.68	0.25 days	
			(b)
Model T-1			
©sum_pr	19.56	118.01 mm	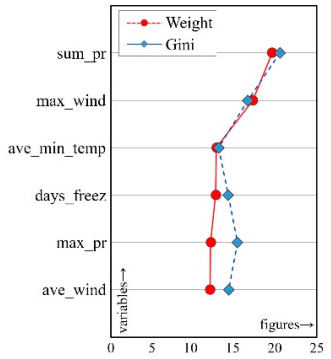
©max_gale	17.22	7.29 m/s	
©ave_mintemp	12.81	28.12 ℃	
©days_freez	12.72	54.05 days	
©max_pr	12.12	86.59 mm	
©ave_gale	12.04	5.25 m/s	
			(c)

3.3. Future building damage predictions

3.3.1. Risk assessment based on weights and limit values

The weights and limit values based on the weather factors that contributed to building damage caused by natural disasters were derived using the decision tree model in section 3.2. According to these results, a risk assessment was conducted for the 230 regions in Korea using climate change scenarios based on the same weather indices to evaluate the risk of building damage in the future.

Observation weather data in South Korea were used for the past building risk assessment (2005–2014), whereas weather data based on climate change scenarios (RCPs 2.6, 4.5, 6.0, and 8.5) from 2021 until 2100 were applied to predict future risks. For the future prediction assessment, the time period was divided into short-term (2021–2040), medium-term (2041–2070), and long-term (2071–2100).

In the assessment method, the value was converted according to the weight of each weather index derived from the decision tree models R-1, S-1, and T-1. The converted score (total score of 100 points) was generated by applying a weight in the regions above the limit value to calculate the risk index in the 230 regions. Regions with a risk index below 20 points were classified as 'very low risk', whereas 20–40 points represented 'low risk', 40–60 points represented 'medium risk', 60–80 points represented 'high risk', and above 80 points represented 'extreme risk'.

3.3.2. Prediction of future buildings damage risk

Figure 7 shows the risk of building damage according to each district in Korea. Figures 8(a)–(c) show the building damage risk in the 230 regions in the past (2005–2014), and Figures 8(d)–(f) show the predicted future risk based on the climate change scenarios. In total, 131 regions were at risk of flood damage in the past (risk index > 40). These regions were concentrated in the northern region (Seoul, Gyeonggi, etc.) and southern region (parts of Gyeongnam and Jeonnam). In addition, 41 regions were at risk of snowfall damage, which were concentrated in the coastal areas of Honam, Gangwon, and Hoseo. Finally, 78 regions were at risk of typhoon damage, which were located mainly in the southern coastal region.

Based on the results using the same method to predict future building damage (2021–2100), an increase in regions at risk of flood damage was found under all climate scenarios (RCPs 2.6, 4.5, 6.0, and 8.5) from 2021 to 2100. The risk of flood damage increased in 224 regions compared to the risk in the past. The predicted increase in flood damage could be due to predicted increases in precipitation in the future. In the case of snowfall, fewer than five regions were predicted to be damaged in the future, indicating a very low risk. This could be explained by the fact that the snowfall for the indices 'sum_nsnd', 'ave_nsnd', and 'max_nsnd' tended to be much lower in the future compared to the past. Finally, areas with damage caused by typhoons were reduced by half compared to the past, except for RCP 6.0 (long-term) and RCP 8.5 (short-, medium- and long-term). In the case of typhoons, a risk assessment was conducted by considering both precipitation and gale speed indices. Higher precipitation was predicted for the future compared to the past, but the gale speeds of 'ave_wind' and 'max_wind' were found to be lower.

Preprints (www.preprints.org) | NOT PEER-REVIEWED | Posted: 12 February 2018 doi:10.20944/preprints201802.0087.v1

Peer-reviewed version available at Sustainability 2018, 10, 1072; doi:10.3390/su10041072

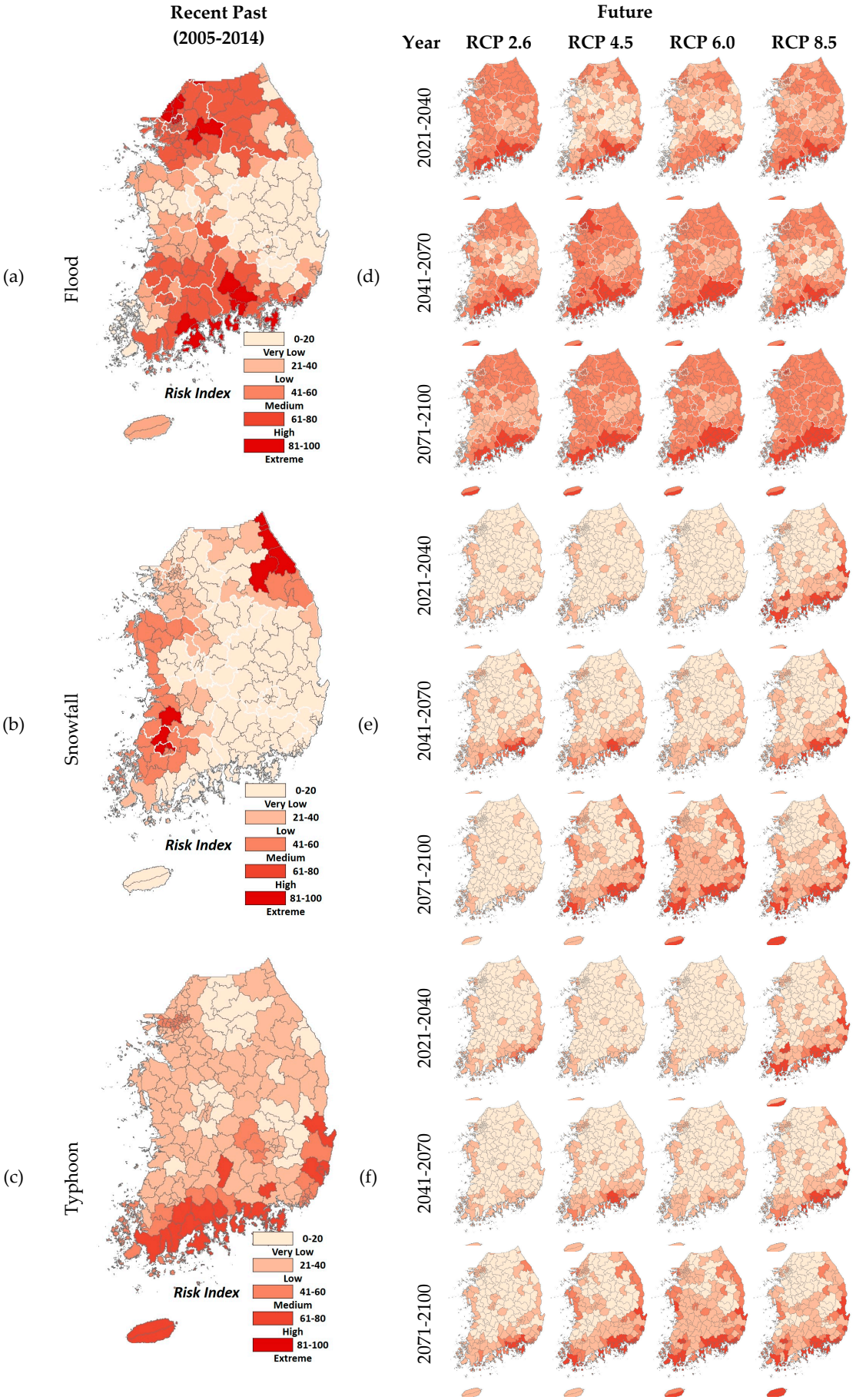

Figure 7. Map of building damage risk (2021–2100)

4. Discussion

In this study, the weights and limit values of building damage were derived using weather indices based on past observation weather data and building damage history to evaluate the risk of building damage caused by natural disasters. Furthermore, the building damage risks for the 230 regions of South Korea were predicted and analyzed based on climate scenarios using the derived indices. As a data mining technique, decision tree analysis was used to determine the weights and limit values according to weather indices. A total of 37 indices were used to construct the input model, while 33 weather indices were applied as independent variables and 4 damage history indices were used as dependent variables.

In the first stage of this research, to assess the building risk in the 230 regions of Korea, a correlation analysis was conducted based on the type of natural disaster (flood, gale, snowfall, and typhoon) to select the variables with the highest correlations to building damage. The input variables for the decision tree model were based on flood, snowfall, and typhoon damage, and the uncorrelated gale damage variable was excluded.

Second, the model with the highest accuracy was selected based on the number of building classifications. The weights according to each weather factor were derived using the decision tree models R-1, S-1, and T-1 as the most accurate models. The weather variables with the highest impact on building damage caused by flood followed the order 'ave_gt80' > 'sum_pr' > 'sum_jja_pr' > 'px5d' > 'max_pr'. The impact building damage caused by snowfall followed the order of 'sum_nsnd' > 'ave_nsnd' > 'max_nsnd' > 'days_nsnd5'. Finally, the impact typhoon building damage followed the order '©sum_pr' > '©max_gale' > '©ave_min_temp' > '©days_freez' > '©max_pr' > '©ave_wind'.

Third, the regions at risk of building damage were predicted for each climate change scenario (RCPs 2.6, 4.5, 6.0, and 8.5). Predictions for multiple time periods (short-, medium- and long-term) were calculated using the limit value according to the building damage category in the decision tree model. The results showed an average increase of over 30% in regions at risk of flood damage (regions with risk indices > 40) compared to the past trends (2005–2014). Conversely, the risk of snowfall damage decreased by more than 90% relative to past trends. There was an average decrease of 57.5% in areas at risk of typhoon damage, but the high risk of typhoon damage (regions with risk indices > 60) increased by more than 60% in RCP 8.5 (see Figure 8).

This study investigated the effects of weather conditions on building damage and predicted future building damage risk using a decision tree analysis for 230 regions in South Korea until 2100. From this analysis, the importance and the damage limit value of the weather variables affecting the building damage were derived. The results support the use of the model presented herein as a stable disaster management technique in the face of uncertain risks caused by natural disasters. The quantitative data used in study can be used to prepare for risks and damage associated with future natural disasters. We expect that this method can be adopted as a main evaluation technique for sustainable growth in Korea. In addition, this study confirmed possibility of using decision tree analysis to evaluate building damage risk. A more accurate disaster prediction model will be constructed in future studies by expanding the input variables and diversifying the analysis techniques.

Preprints (www.preprints.org) | NOT PEER-REVIEWED | Posted: 12 February 2018 doi:10.20944/preprints201802.0087.v1

Peer-reviewed version available at Sustainability 2018, 10, 1072; doi:10.3390/su10041072

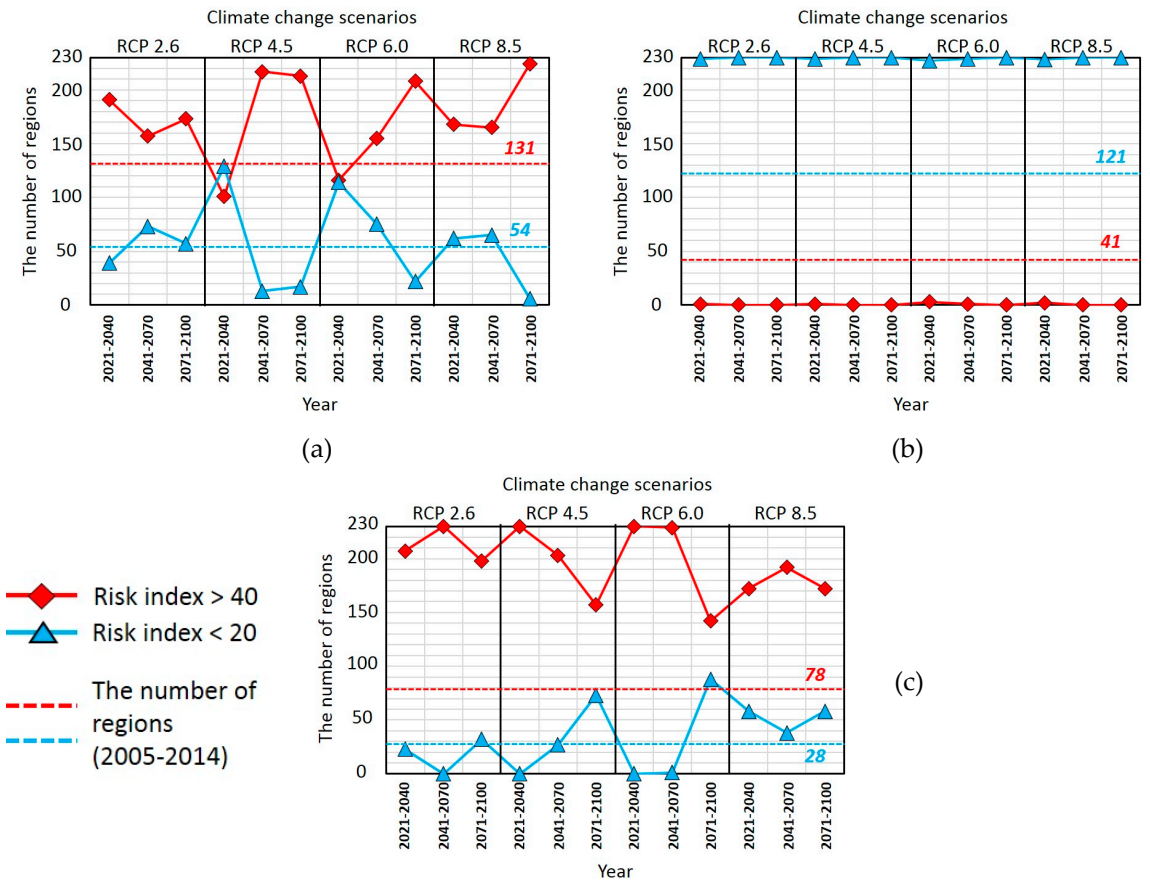

Figure 8. Assessment of building damage risk by regions from 2021-2100 : (a) Flood; (b) Snow; (c) Typhoon.

Acknowledgments: This research was supported by Basic Science Research Program through the National Research Foundation of Korea(NRF) funded by the Ministry of Education(NRF-2017R1E1A1A01074904).

Author Contributions: Keum Ji Kim analyzed the data and designed the research. Seong Hwan Yoon supported and supervised the research. Keum Ji Kim and Seong Hwan Yoon conceived and designed the research.

Conflicts of Interest: The authors declare no conflict of interest.

References

1. *Climate change 2014-synthesis report*; Intergovernmental Panel of Climate Change: 2014; pp 1-2.
2. Hardy, J.T. *Climate change: Causes, effects, and solutions*. WILEY, 2003.
3. *Annual disaster statistical review 2016(the numbers and trends)*; The Centre for Research on the Epidemiology of Disasters: 2017; pp 1-80.
4. Laframboise, N.; Loko, B. *Natural disasters: Mitigating impact, managing risks*; International Monetary Fund: 2012.
5. *Overview of natural disasters and their impacts in asia and the pacific 1970-2014*; Economic and Social Commission for Asia and the Pacific: 2015; pp 1-32.
6. Mirza, M.M.Q. Climate change and extreme weather events: Can developing countries adapt? *Climate Policy* **2003**, *3*, 233-248.
7. Disasters in asia and the pacific_2015 year in review. *Economic and Social Commission for Asia and the Pacific* **2015**, 1-21.
8. RĂDulescu, C.V.; Ioan, I.; Andreica, M. In *International mechanism for loss and damage caused by climate change*, 2016; pp 82-85.

9. Blong, R. Residential building damage and natural perils: Australian examples and issues. *Building Research & Information* **2004**, *32*, 379-390.
10. Chandler, A.M.; Jones, E.J.W.; Patel, M.H. Property loss estimation for wind and earthquake perils. *Risk Analysis: An International Journal* **2001**, *21*, 235-250.
11. Konukcu, B.; Karaman, H.; Şahin, M. Building damage analysis for the updated building dataset of istanbul. *Natural Hazards* **2016**, *84*, 1981-2007.
12. Yazdani, N.; Dowgul, R.W.; Manzur, T. Deficiency analysis of coastal buildings toward storm damage reduction. *Journal of Performance of Constructed Facilities* **2010**, *24*, 128-137.
13. Luo, J.; Liang, D.; Weiss, C. Reconstruction of a near-surface tornado wind field from observed building damage. *Wind & structures* **2015**, *20*, 389-388.
14. Pita, G.; Pinelli, J.P.; Cocke, S.; Gurley, K.; Mitrani-Reiser, J.; Weekes, J.; Hamid, S. Assessment of hurricane-induced internal damage to low-rise buildings in the florida public hurricane loss model. *Journal of Wind Engineering & Industrial Aerodynamics* **2012**, *104-106*, 76-87.
15. Atillah, A.; El Hadani, D.; Moudni, H.; Lesne, O.; Renou, C.; Mangin, A.; Rouffi, F.; Didenkulova, I.; Dominey-Howes, D.; Papathoma-Koehle, M.*, et al.* Tsunami vulnerability and damage assessment in the coastal area of rabat and salé, morocco. *Natural Hazards & Earth System Sciences* **2011**, *11*, 3397-3414.
16. Cole, S.W.; Xu, Y.; Burton, P.W. Seismic hazard and risk in shanghai and estimation of expected building damage. *Soil Dynamics & Earthquake Engineering (0267-7261)* **2008**, *28*, 778-794.
17. Nadal, N.C.; Zapata, R.E.; Pagán, I.; López, R.; Agudelo, J. Building damage due to riverine and coastal floods. *Journal of Water Resources Planning & Management* **2010**, *136*, 327-336.
18. José María, B.; Carolina, G.-A.; Estefanía, A.-J.; Miguel Ángel, E.; María Lorena, M.-C. Flood damage analysis: First floor elevation uncertainty resulting from lidar-derived digital surface models. *Remote Sensing, Vol 8, Iss 7, p 604 (2016)* **2016**, *8*, 604-604.
19. Unnikrishnan, V.U.; Barbato, M. Performance-based comparison of different storm mitigation techniques for residential buildings. *Journal of Structural Engineering* **2016**, *142*, 1-12.
20. Goswami, S.; Chakraborty, S.; Ghosh, S.; Chakrabarti, A.; Chakraborty, B. A review on application of data mining techniques to combat natural disasters. *Ain Shams Engineering Journal* **2016**, 1-14.
21. Chen, S.; Wang, Y.; Tsou, I. Using artificial neural network approach for modelling rainfall-runoff due to typhoon. *Journal of Earth System Science* **2013**, *122*, 399-405.
22. Radhika, S.; Tamura, Y.; Matsui, M. Cyclone damage detection on building structures from pre- and post-satellite images using wavelet based pattern recognition. *Journal of Wind Engineering and Industrial Aerodynamics* **2015**, *136*, 23-33.
23. Fawzy, D.E.; Arslan, G. Development of building damage functions for big earthquakes in turkey. *Procedia - Social and Behavioral Sciences* **2015**, *195*, 2290-2297.
24. Tehrany, M.S.; Pradhan, B.; Jebur, M.N. Flood susceptibility mapping using a novel ensemble weights-of-evidence and support vector machine models in gis. *Journal of Hydrology* **2014**, *512*, 332-343.
25. Liu, Y.; Li, L.; Chen, Q.; Shu, M.; Zhang, Z.; Liu, X. In *Building damage assessment of compact polarimetric sar using statistical model texture parameter*, 2017; IEEE: pp 1-4.
26. Reese, S.; Bradley, B.A.; Bind, J.; Smart, G.; Power, W.; Sturman, J. Empirical building fragilities from observed damage in the 2009 south pacific tsunami. *Earth-Science Reviews* **2011**, *107*, 156-173.

27. Easterling, D.R.; Meehl, G.A.; Parmesan, C.; Changnon, S.A.; Karl, T.R.; Mearns, L.O. Climate extremes: Observations, modeling, and impacts. *science* **2000**, *289*, 2068-2074.
28. Spekkers, M.H.; Clemens, F.H.L.R.; Veldhuis, J.A.E.t. On the occurrence of rainstorm damage based on home insurance and weather data. *Natural Hazards and Earth System Sciences, Vol 15, Iss 2, Pp 261-272 (2015)* **2015**, *15*, 261-272.
29. Tamura, H.; Yamamoto, K.; Tomiyama, S.; Hatono, I. Modeling and analysis of decision making problem for mitigating natural disaster risks. *European Journal of Operational Research* **2000**, *122*, 461-468.
30. Ragettli, S.; Zhou, J.; Wang, H.; Liu, C.; Guo, L. Research papers: Modeling flash floods in ungauged mountain catchments of china: A decision tree learning approach for parameter regionalization. *Journal of Hydrology* **2017**, *555*, 330-346.
31. Wang, Z.; Lai, C.; Chen, X.; Yang, B.; Zhao, S.; Bai, X. Flood hazard risk assessment model based on random forest. *Journal of Hydrology* **2015**, *527*, 1130-1141.
32. Quanlong, F.; Jianhua, G.; Jiantao, L.; Yi, L. Flood mapping based on multiple endmember spectral mixture analysis and random forest classifier-the case of yuyao, china. *Remote Sensing* **2015**, *7*, 12539-12562.
33. Yan-yan, S.; Ying, L.U. Decision tree methods: Applications for classification and prediction. *Shanghai Archives of Psychiatry* **2015**, *27*, 130-135.
34. Friedl, M.A.; Brodley, C.E. Decision tree classification of land cover from remotely sensed data. *Remote Sensing of Environment* **1997**, *61*, 399-409.
35. Rules generation from the decision tree. *JOURNAL OF INFORMATION SCIENCE AND ENGINEERING* **2001**, *17*, 325-340.
36. Kim, K.-J.; Seo, J.-B.; Yoon, S.-H. Analysis and prediction of urban thermal environment using rcp scenarios. *Journal of the Regional Association of Architectural Institute of Korea* **2017**, *19*, 107-114.
37. Prasad, N.; Patro, K.R.; Naidu, M.M. In *A gini index based elegant decision tree classifier to predict precipitation*, 2013; IEEE: pp 46-54.
38. Gislason, P.O.; Benediktsson, J.A.; Sveinsson, J.R. Random forests for land cover classification. *Pattern Recognition Letters* **2006**, *27*, 294-300.
39. Quanlong, F.; Jiantao, L.; Jianhua, G. Urban flood mapping based on unmanned aerial vehicle remote sensing and random forest classifier-a case of yuyao, china. *Water* **2015**, *7*, 1437-1455.
40. Lai, C.; Shao, Q.; Chen, X.; Wang, Z.; Zhou, X.; Yang, B.; Zhang, L. Flood risk zoning using a rule mining based on ant colony algorithm. *Journal of Hydrology* **2016**, *542*, 268-280.
41. *The fourth national comprehensive plan-revision plan (2011-2020)*. Republic of Korea, 2011; p 1-183.
42. Kim, G.; Cha, D.; Lee, G.; Jin, C.; Lee, D.; Suh, M.; Ahn, J.; Min, S.; Hong, S.; Kang, H. Impact of horizontal resolution on precipitation simulation over south korea with multi regional climate models. *Journal of Climate Research* **2016**, *11*, 169-181.
43. Arnell, N.W.; Hudson, D.A.; Jones, R.G. Climate change scenarios from a regional climate model: Estimating change in runoff in southern africa. *Journal of Geophysical Research: Atmospheres* **2003**, *108*.
44. Kim, J.; Kim, T.; Lee, B. An analysis of typhoon damage pattern type and development of typhoon damage forecasting function. *Korean Society of Hazard Mitigation* **2017**, *17*, 339-347.
45. *A study on enhancing the community capacity for hazard mitigation in climate change*; Ministry of the Interior and Safety: 2017.

611 46. Suh, M.S.; Oh, S.G.; Lee, D.K.; Cha, D.H.; Choi, S.J.; Jin, C.S.; Hong, S.Y. Development of new
612 ensemble methods based on the performance skills of regional climate models over south korea.
613 *Journal of climate* **2012**, *25*, 7067-7082.
614 47. Kim, G.; Kim, J.; Kim, C.; Jin, C.; Cha, D.; Suh, M.; Park, S. Climate change projections over cordex
615 east asia domain using multi-rcms. *Journal of Climate Research* **2014**, *9*, 257-268.
616 48. Teutschbein, C.; Seibert, J. Bias correction of regional climate model simulations for hydrological
617 climate-change impact studies: Review and evaluation of different methods. *Journal of Hydrology*
618 **2012**, *456-457*, 12-29.